Travelling waves for an epidemic model with nonsmooth treatment rates

N. Hussaini and M. Winter *
Department of Mathematical Sciences, Brunel University, West London, UB8 3PH, UK

Abstract

We consider a Susceptible-Infected-Removed (SIR) epidemic model with two types of nonlinear treatment rates: (i) piecewise linear treatment rate with saturation effect, (ii) piecewise constant treatment rate with a jump (Heaviside function). For Case (i), we compute travelling front solutions whose profiles are heteroclinic orbits which connect either the disease-free state to an infective state or two endemic states with each other. For Case (ii), it is shown that the profile has the following properties: the number of susceptibles is monotone increasing and the number of infectives approaches zero at infinity, while their product converges to a constant. Numerical simulations are performed for all these cases. Abnormal behaviour like travelling waves with non-monotone profile or oscillations are observed.

Keywords: population dynamics (theory), population dynamics (experiment), dynamics (theory), epidemic modelling

1 Introduction

Since the pioneering work of Kermack and McKendrick [1] in 1927, mathematical epidemiology developed an extensive body of literature and SIR models have been playing an important role in modelling epidemics of infectious diseases (such as measles, chickenpox, SARS, HIV, flu and poliomyelitis). The SIR model is suitable for: (i) directly transmitted diseases such as measles, rubella, or mumps, for which an infection confers permanent immunity (i.e., the individual once recovered is not susceptible to infection again) [2, 3, 4], (ii) diseases that allow the permanent removal of some of the

*Corresponding author Email: *matthias.winter@brunel.ac.uk*

infectives from the infectious class due to quarantine, isolation, treatment, etc [5, 8, 34]. Many researchers have studied the classical SIR model (e.g., [5, 8, 10, 14, 17] and the references therein), which describes the infection and removal process of individuals during an epidemic of an infectious disease. The SIR model is one of the simplest and yet most accurate of all biological models [6, 7]. Deterministic models for studying dynamics of epidemics are based on ordinary differential equations.

In recent years, some mathematical models incorporating treatment have been studied by many researchers (e.g., [5, 10, 32, 33, 34]). We define treatment as a way of dealing with a patient medically which may include isolation or quarantine. Further, treatment is an important method to reduce the burden and spread of diseases such as AIDS, TB, and SARS [35, 36, 37, 38]. Thus, in this paper, infective individuals are removed from the infective class due to the treatment at a certain rate.

In mathematical epidemiology, some models for spatial spread of epidemics have been analyzed [18, 19, 21, 27, 28, 40, 41, 46]. A fascinating question is whether a disease could remain endemic by the geographic motion of individuals. Mobility formulation as a random diffusion process in epidemic models takes the form of reaction-diffusion equations, which have been successful in modelling the spatial spread of diseases as illustrated in [18]. In the theory of reaction-diffusion equations, travelling waves play an important role and many techniques have been developed to prove existence or stability of such waves (see, e.g., [20], [22],[23] and [30] for their existence, and stability results can be found in [26], [29] and references therein). In general, Murray [18], Gardner [15], Fife [16] and Volpert *et al.* [26] provide a great detail on the subject. The investigations on travelling wave solutions for epidemic models are attracting more and more attention [19].

In this paper, we consider epidemiological models introduced in [5] and [10] which have certain non-smooth nonlinearities. After adding diffusion terms to the system like in [9], we analyze travelling-wave solutions. We consider two different cases for nonlinear and non-smooth treatment terms: (i) piecewise linear treatment rate with saturation effect, (ii) piecewise constant treatment rate with a jump (Heaviside function). In Case (i), we observe some effects which are not present for travelling waves in classical SIR systems with constant coefficients such as non-monotone profiles for both susceptibles and infectives, or oscillations of the profiles due to complex eigenvalues. In

Case (ii), we observe a profile for which the susceptibles tend to infinity, the infectives converge to zero and their product approaches a constant at the forward end of the profile.

Finally, numerical simulations are presented which confirm these analytical results.

The organization of the paper is as follows. In Section 2, the model is introduced, first in its spatially independent then in its spatially dependent form. Then results on its disease-free and endemic equilibria are stated. The existence of travelling wave front solutions are established in Section 3. Finally, we conclude by briefly discussing our results in Section 4.

2 Model

2.1 Basic Model

Following [5, 10], we consider, as basic model, the following deterministic system of nonlinear differential equations which represent an SIR model with nonlinear and non-smooth treatment rate:

$$\begin{aligned} \frac{dS}{dt} &= A - dS - \lambda SI, \\ \frac{dI}{dt} &= \lambda SI - dI - T(I), \\ \frac{dR}{dt} &= T(I) - dR, \end{aligned} \tag{1}$$

where $S(t)$, $I(t)$ and $R(t)$ denote three classes, namely, susceptible to disease, infective and infectious, and removed (infective, but no longer infectious due to treatment) individuals at time t, respectively. The constant A is the recruitment rate of the population, d the natural death rate of the population and λ the force of infection associated with the transmission of the disease from susceptibles to infectives, $T(I)$ is the treatment rate of infective individuals. In most epidemic models it is assumed that $T(I) = cI$ for some constant $c > 0$. To take into account the limited capacity of treatment facilities, Wang [10] considers a treatment rate which is proportional to the number of the infectives below the maximal capacity and remains constant otherwise. Furthermore, Wang and Ruan [5] adopted a piecewise constant treatment rate with a

jump. Thus, we consider both cases with regard to the definition of $T(I)$ as follows:

$$(i) \quad T(I) = \begin{cases} rI, & \text{if } 0 \leq I \leq I_0, \\ \\ k, & \text{if } I > I_0, \end{cases} \qquad (ii) \quad T(I) = \begin{cases} 0, & \text{if } I \leq 0, \\ \\ m, & \text{if } I > 0, \end{cases} \tag{2}$$

as defined in [5] and [10] respectively, where the constants $r > 0$, $m > 0$, $k = rI_0$ and I_0 is the capacity of treatment resources. Note that for (i) we have a piecewise linear treatment rate with saturation effect and for (ii) a piecewise constant treatment rate with jump (Heaviside function). Epidemiologically, case (i) is more appropriate if medicines to be supplied to the infectives are not sufficient or in a case where the number of hospital beds is limited. Case (ii) is valid for the situation where the population of the infectives is much more than the resources available for the treatment. Thus, the maximum capacity of the treatment is reached instantly.

Nonlinear incidence rates of different types have been used in many epidemiological models (e.g., [43, 44, 45, 46] and the references therein). However, in classical epidemic models, the incidence rate (the rate of new infections) is bilinear $\lambda\, S\, I$ or standard $\dfrac{\lambda\, S\, I}{N}$. The bilinear incidence rate is more suitable for communicable diseases such as SARS, swine flu, etc., but not for sexually transmitted diseases like HIV, whilst standard incidence rate is more appropriate if the number of available partners is large enough and everybody could not make more contacts than is practically feasible [5].

2.2 Spatial SIR Model

We now add diffusion effects to the basic model as in [9]. Whereas [9] analyze Turing instability and simulate stripy patterns, we are interested in travelling waves.

Random movement of individuals in space was further incorporated into model (1) by adding some diffusion terms, so that Fick's law holds. Letting $S(x,t)$ and $I(x,t)$ be the respective densities at a spatial position x and time t, this results in the following system of PDEs:

$$S_t = A - d\, S - \lambda S\, I + D_s\, S_{xx}, \tag{3a}$$

$$I_t = \lambda S\, I - d\, I - T(I) + D_i\, I_{xx}, \tag{3b}$$

$$R_t = T(I) - d\, R + D_r\, R_{xx}, \qquad x \in \mathbb{R}, \quad t > 0, \tag{3c}$$

where D_s, D_i and D_r are the diffusion rates for the susceptible, infective and recovered individuals, respectively. Since the first two equations of system (3) are independent of the last one, it suffices to consider the following reduced reaction diffusion model:

$$\begin{aligned} S_t &= A - d\,S - \lambda S\,I + D_s\,S_{xx}, \\ I_t &= \lambda S\,I - d\,I - T(I) + D_i\,I_{xx}, \qquad x \in \mathbb{R}, \quad t > 0. \end{aligned} \tag{4}$$

After solving system (4), R can be determined from (3c) which is a linear equation for R. It is assumed that the parameters A, d, λ, D_s, D_i are all positive constants. The system (4) has a disease-free equilibrium $\mathcal{E}_0 = (A/d, 0)$. For Case (i), the basic reproduction numbers are given by $\mathcal{R}_0 = \dfrac{\lambda A}{d(d+r)}$ if $0 \le I \le I_0$ and $\mathcal{R}'_0 = \dfrac{\lambda A}{d^2}$ if $I > I_0$, which measure the average number of new infections generated by a single infective person in a community. For Case (ii), $\mathcal{R}'_0$ is always used. Note that $\mathcal{R}_0 = \dfrac{\lambda A}{d(d+r)} < \mathcal{R}'_0 = \dfrac{\lambda A}{d^2}$. The number of infective individuals is expected to decline towards zero whenever $\mathcal{R}'_0 < 1$, because each infective individual on average infects less than one susceptible person. The disease will persist whenever $\mathcal{R}_0 > 1$.

We now consider homogeneous equilibria of system (4). For Case (i) there will be a positive endemic equilibrium $\mathcal{E}_1 = (S_1, I_1)$ of the system (4) provided $1 < \mathcal{R}_0 \le 1 + \dfrac{\lambda\,k}{d\,r}$, where

$$S_1 = \frac{d+r}{\lambda}, \qquad I_1 = \frac{d(\mathcal{R}_0 - 1)}{\lambda} < I_0.$$

Further, define $b = d^2 + (k - A)\,\lambda$ and $\Delta = b^2 - 4\,d^2\,k\,\lambda$. Following [10], if $\Delta \ge 0$ then we have positive endemic equilibria of system (4), namely, $\mathcal{E}_2 = (S_2, I_2)$ and $\mathcal{E}_3 = (S_3, I_3)$, where

$$S_2 = \frac{A}{(d + \lambda I_2)}, \qquad I_2 = \frac{-b - \sqrt{\Delta}}{2d\lambda} > I_0,$$

$$S_3 = \frac{A}{(d + \lambda I_3)}, \qquad I_3 = \frac{-b + \sqrt{\Delta}}{2d\lambda} > I_0.$$

From Theorems 2.1 and 2.2 of [10], we deduce the following result.

Proposition 1. *Consider the system (4), where $T(I)$ is given by Case (i), and define $p_0 = 1 + \dfrac{\lambda\,k - d\,r}{d(d+r)} + \dfrac{2\sqrt{\lambda\,k}}{(d+r)}$, $p_1 = 1 + \dfrac{\lambda\,k - d\,r}{d(d+r)} + \dfrac{2\lambda\,k}{r(d+r)}$ and $p_2 = 1 + \dfrac{\lambda\,k}{d\,r}$. Suppose that $\mathcal{R}_0 \ge p_0$ and $\mathcal{R}_0 > 1$ then*

(a) $\mathcal{E}_1$ is the unique endemic equilibrium if $\mathcal{R}_0 \le p_2$ and $\mathcal{R}_0 < p_1$.

(b) The endemic equilibrium points $\mathcal{E}_2$ and $\mathcal{E}_3$ co-exist whenever $p_1 < \mathcal{R}_0 < p_2$.

We will investigate travelling wave solutions whose profiles are heteroclinic orbits connecting different equilibrium points of system (4) in Section 3.

2.3 Stability of Disease-free Equilibrium

Here, we are concerned with the stability of the disease-free equilibrium $\mathcal{E}_0 = (A/d, 0)$ of the system (4). Therefore, we claim the following result.

Theorem 1. *Suppose that $\mathcal{R}_0 < 1$ in the system (4), where the nonlinearity $T(I)$ is given in Case (i) of equation (2). Then the disease-free equilibrium $\mathcal{E}_0 = (A/d, 0)$ is locally asymptotically stable.*

Proof. Consider the vector field

$$(f_1(S,I), f_2(S,I)) = (S\,M(S,I), I\,N(S,I)),$$

where

$$f_1(S,I) = A - d\,S - \lambda S\,I, \quad f_2(S,I) = \lambda S\,I - d\,I - T(I),$$

$$M(S,I) = A/S - d - \lambda I \quad \text{and} \quad N(S,I) = \lambda S - d - T(I)/I.$$

Note that $M_I(S,I) < 0$ and $N_S(S,I) > 0$ (where subscripts denote differentiation). The Jacobian J of the vector field $(S\,M(S,I), I\,N(S,I))$ around the disease-free equilibrium $\mathcal{E}_0$ is given by

$$J = \begin{pmatrix} -d & -\frac{\lambda A}{d} \\ 0 & \frac{\lambda A}{d} - (d+r) \end{pmatrix}.$$

Thus, the eigenvalues of J are both negative if $\mathcal{R}_0 < 1$. From Theorem 4.1 of [24], there exists an open neighourhood Σ of $\mathcal{E}_0$ which is contained in

$$\{(S,I) :\ S \geq 0,\ I \geq 0\}$$

such that every solution to the system (4) with initial conditions in Σ decays exponentially to $\mathcal{E}_0$ as $t \to \infty$. □

Under slightly stronger assumptions (replacing $\mathcal{R}_0 < 1$ by $\mathcal{R}_0' < 1$) we are able to prove a result which includes both Cases (i) and (ii) for $T(I)$ and explicitly locates a set of initial conditions for which asymptotic stability holds.

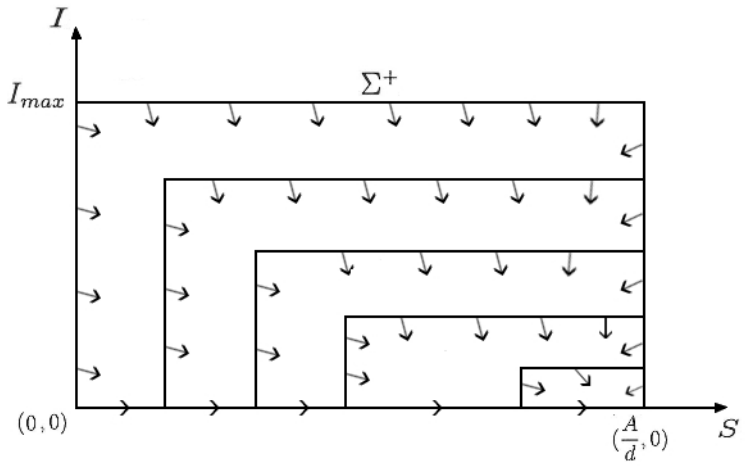

Figure 1: semi-contracting rectangle

Theorem 2. *Suppose that* $\mathcal{R}_0' < 1$*, then the disease-free equilibrium* $\mathcal{E}_0 = (\frac{A}{d}, 0)$ *of the system (4) is locally asymptotically stable. More precisely,* $(S(t,x), I(t,x)) \to (\frac{A}{d}, 0)$ *if* $(S(0,x), I(0,x)) \in \Sigma^+$ *where* $\Sigma^+ = (0, \frac{A}{d}) \times (0, I_{max})$ *for all* $x \in \mathbb{R}$*, and* $I_{max} = \frac{d}{2\lambda}$.

Proof.

Consider the rectangle $\Sigma^+ = (0, \frac{A}{d}) \times (0, I_{max})$ given in Figure 1, where $I_{max} = \frac{d}{2\lambda}$.

Let $f_1(S,I) = A - d\,S - \lambda S\,I$ and $f_2(S,I) = \lambda S\,I - d\,I - T(I)$. We can easily see that f_1 is negative on the "right edge" of Σ^+, and positive on the "left edge" of Σ^+. On the other hand, on the "top" of Σ^+,

$$f_2(S, I_{max}) = \lambda S\,I_{max} - d\,I_{max} - T(I_{max}).$$

Since $S \leq \frac{A}{d}$ and $\mathcal{R}_0' < 1$ then $f_2(S, I_{max}) < 0$. On the "bottom" of Σ^+, $f_2(S,0) = 0$. Thus, Σ^+ is a semi-contracting rectangle as defined in [31].

In the same way we now show that

$$\gamma\Sigma^+ + (1-\gamma)(\frac{A}{d}, 0) = [(1-\gamma)\frac{A}{d}, \frac{A}{d}] \times [0, \gamma I_{max}] := [S_l, \frac{A}{d}] \times [0, I_l]$$

is a family of similar semi-contracting rectangles for $0 < \gamma < 1$ centered at the point $(\frac{A}{d}, 0)$. By definition, it is clear that this is a similar family of rectangles. Further, as

in the case $I_l = I_{max}$, this is a semi-contracting family if

$$A - d\,S_l - \lambda S_l\,I_l > 0, \tag{5}$$

where $S_l = (1-\gamma)\frac{A}{d}$ and $I_l = \gamma I_{max}$ for all $0 < \gamma < 1$. From (5), we obtain

$$\frac{\lambda(1-\gamma)}{d} I_{max} < 1 \quad \text{for all } 0 \leq \gamma \leq 1.$$

The condition (5) is satisfied if $I_{max} < \frac{d}{\lambda}$. Choosing $I_{max} = \frac{d}{2\lambda}$, we have a similar semi-contracting family of rectangles centered at $(\frac{A}{d}, 0)$.

Finally, by using the same argument as in the proof of Lemma 3.8 of [29], the result follows. □

Remarks:

(1) Theorem 1 considers the nonlinearity in Case (i) of equation (2) only, while Theorem 2 deals with both nonlinearities of equation (2).

(2) It is assumed that $\mathcal{R}_0 < 1$ and $\mathcal{R}_0^{'} < 1$ in Theorems 1 and 2, respectively, where $\mathcal{R}_0 < \mathcal{R}_0^{'} < 1$. Thus, the condition in Theorem 2 is stronger.

(3) Σ^+ is located to the left of the point $(\frac{A}{d}, 0)$ in Theorem 2, whilst there exists Σ around $(\frac{A}{d}, 0)$ in Theorem 1.

(4) Mulone *et al.* introduced Liapunov functions to prove nonlinear stability of some epidemic models of SI type [40]. Their method is elegant and shows global stability, but it requires special transformations and works only on bounded domains.

3 Travelling-wave solutions

The spatial model (4) is the starting point of the analysis in this paper. We are interested in the question of the existence of travelling wave solutions. Now, we look for travelling wave solutions of the form $S(x,t) = u(x+ct) = u(z)$ and $I(x,t) = v(x+ct) = v(z)$ with $z = x + ct$ and c is the travelling wave speed. We assume that susceptible individuals and infectives diffuse at the same rate (i.e., $D_s = D_i = 1$) and substitute u and v into (4). These result in the following coupled system of ordinary

differential equations:

$$u_{zz} - cu_z + A - du - \lambda uv = 0, \tag{6a}$$

$$v_{zz} - cv_z + \lambda uv - dv - T(v) = 0. \tag{6b}$$

Biologically speaking, the introduction of few infective individuals at one end of a linear habitat (e.g., coastline), which is initially uniformly saturated with susceptible individuals at the carrying capacity of the environment, may result in a "wave of propagation" of infective individuals. Therefore, a zone of transition from one equilibrium point to another is possible and the travelling wave profile occurs when this transition zone moves across the population [23]. In order to investigate the existence of such a travelling wave of system (4), let $f = u_z$ and $g = v_z$, so that $f_z = u_{zz}$ and $g_z = v_{zz}$, which leads to the four-dimensional system

$$u_z = f, \tag{7a}$$

$$f_z = c\,f - A + d\,u + \lambda\,u\,v, \tag{7b}$$

$$v_z = g, \tag{7c}$$

$$g_z = c\,g - \lambda\,u\,v + d\,v + T(v). \tag{7d}$$

Now we state the following Corollary about the non-existence of certain travelling waves which follows immediately from Theorem 2.

Corollary 1. *Suppose that $\mathcal{R}_0^{'} < 1$, then there is no travelling wave profile from the disease-free equilibrium $\mathcal{E}_0 = (\frac{A}{d}, 0)$ of the system (6) provided the initial sizes of the sub-populations are within the semi-contracting set $\Sigma^+ = (0, \frac{A}{d}) \times (0, I_{max})$.*

Proof. Corollary 1 follows directly from the result of Theorem 2. □

In the following subsections, we consider the Case (i) piecewise linear treatment rate with saturation effect and Case (ii) piecewise constant treatment rate with jump separately.

3.1 Piecewise linear treatment rate with saturation effect

In this section, we assume that the treatment rate is proportional to the number of infectives when the capacity of treatment is less than or equal to the number of infective

individuals and takes the maximal capacity otherwise (i.e., we are considering Case (i)). We shall first establish the existence of a heteroclinic connection in $\mathbb{R}^4$. In other words, a travelling wave solution must correspond to a trajectory that connects two different steady states in $\mathbb{R}^4$. A travelling wave solution of system (4) exists if there is a heteroclinic orbit connecting at least two of the following critical points of (7), which are related to the equilibrium point found in Section 2.2.

$$\mathcal{E}'_0 = \begin{pmatrix} 0 \\ A/d \\ 0 \\ 0 \end{pmatrix}, \qquad \mathcal{E}'_1 = \begin{pmatrix} 0 \\ S_1 \\ 0 \\ I_1 \end{pmatrix}, \qquad \mathcal{E}'_2 = \begin{pmatrix} 0 \\ S_2 \\ 0 \\ I_2 \end{pmatrix} \qquad \text{and} \qquad \mathcal{E}'_3 = \begin{pmatrix} 0 \\ S_3 \\ 0 \\ I_3 \end{pmatrix}.$$

Linearization of (7) about $\mathcal{E}'_0$ has a characteristic equation

$$\lambda^4 - 2\,c\lambda^3 + \frac{(-2\,d^2 - rd + \lambda\,A + c^2 d)\,\lambda^2}{d} - \frac{c\,(-2\,d^2 - rd + \lambda\,A)\,\lambda}{d} + d^2 + rd - \lambda\,A = 0.$$

Thus, it has the following eigenvalues

$$\Lambda_{1,2} = \frac{c \pm \sqrt{c^2 + 4\,d}}{2} \qquad \text{and} \qquad \Lambda_{3,4} = \frac{c \pm \sqrt{c^2 - 4(r+d)(\mathcal{R}_0 - 1)}}{2\,d}. \tag{8}$$

Since $\mathcal{R}_0 > 1$, then for $c > c^*$, where $c^* = 2\sqrt{(r+d)(\mathcal{R}_0 - 1)}$, the stable manifold at $\mathcal{E}'_0$, denoted by $\mathcal{M}_s(\mathcal{E}'_0)$, is three dimensional (that is, $\dim(\mathcal{M}_s(\mathcal{E}'_0)) = 3$) while the dimension of the unstable manifold is one (that is, $\dim(\mathcal{M}_u(\mathcal{E}'_0)) = 1$). If $c \geq c^*$ then all the four eigenvalues in equations (8) are real.

However, if $0 < c < c^*$ then Λ_3 and Λ_4 are a pair of complex conjugate eigenvalues with positive real part. From Theorems 6.1 and 6.2 in [39], we have a two-dimensional unstable manifold at $\mathcal{E}'_0$ and the disease-free equilibrium point is a spiral point on this unstable manifold. A trajectory approaching $\mathcal{E}'_0$ must have $v(z) < 0$ for some z. This contradicts the fact that the travelling wave solutions are non-negative. Therefore, c^* is a minimal wave speed.

Hence, we summarize the result as follows.

Theorem 3. *Suppose that $\mathcal{R}_0 > 1$ and $0 < c < c^*$, then the system (7) with Case (i) of equation (2) has no heteroclinic orbit connecting $\mathcal{E}'_0$ with any of the endemic equilibrium points.*

Let $\mathcal{M}_s(\mathcal{E}'_i)$ and $\mathcal{M}_u(\mathcal{E}'_i)$ denote the local stable and unstable manifolds associated with $\mathcal{E}'_i$, $i = 0, 1, 2, 3$. We claim the following result.

Lemma 1. *Suppose that Case (a) of Proposition 1 holds, then*

$$dim(\mathcal{M}_s(\mathcal{E}'_0)) + dim(\mathcal{M}_u(\mathcal{E}'_1)) = dim(\mathbb{R}^4) + 1.$$

Proof. Let Case (a) of Proposition 1 hold, then $\mathcal{E}'_1$ exists and we may linearize (7) around $\mathcal{E}'_1$. Thus, we have the following characteristic polynomial

$$\lambda^4 - 2\,c\lambda^3 + \left(c^2 - d\mathcal{R}_0\right)\lambda^2 + c\,d\mathcal{R}_0\lambda + d\,(\mathcal{R}_0 - 1)\,(d + r) = 0,$$

and the corresponding eigenvalues

$$\Lambda_{1,2} = \frac{c \pm \sqrt{c^2 + 2\,d\mathcal{R}_0 - 2\sqrt{\Delta_2}}}{2},$$

$$\Lambda_{3,4} = \frac{c \pm \sqrt{c^2 + 2\,d\mathcal{R}_0 + 2\sqrt{\Delta_2}}}{2}$$

where $\Delta_2 = d^2{\mathcal{R}_0}^2 - 4\,d(d+r)(\mathcal{R}_0 - 1)$. This implies $\dim(\mathcal{M}_s(\mathcal{E}'_1)) = \dim(\mathcal{M}_u(\mathcal{E}'_1)) = 2$. Since $\dim(\mathcal{M}_s(\mathcal{E}'_0)) = 3$ and $\dim(\mathcal{M}_u(\mathcal{E}'_0)) = 1$, then

$$\dim(\mathcal{M}_s(\mathcal{E}'_0)) + \dim(\mathcal{M}_u(\mathcal{E}'_1)) = \dim(\mathbb{R}^4) + 1.$$

□

Lemma 2. *Suppose that Case (b) of Proposition 1 holds, then*

$$dim(\mathcal{M}_s(\mathcal{E}'_0)) + dim(\mathcal{M}_u(\mathcal{E}'_3)) = dim(\mathbb{R}^4) + 1.$$

Proof. Let Case (b) of Proposition 1 hold, then $\mathcal{E}'_3$ exists. By using similar argument above, we linearize around $\mathcal{E}'_3$ and obtain the following eigenvalues

$$\frac{c \pm \sqrt{c^2 + 4d}}{2} \quad \text{and} \quad \frac{c \pm \sqrt{c^2 + \frac{4}{d}\sqrt{\Delta}}}{2},$$

with $\dim(\mathcal{M}_s(\mathcal{E}'_3)) = \dim(\mathcal{M}_u(\mathcal{E}'_3)) = 2$ where $\Delta = b^2 - 4\,d^2\,k\,\lambda$ and $b = d^2 + (k - A)\,\lambda$. Hence, $\dim(\mathcal{M}_s(\mathcal{E}'_0)) + \dim(\mathcal{M}_u(\mathcal{E}'_3)) = \dim(\mathbb{R}^4) + 1$. □

The Lemmas 1 and 2 show that $\mathcal{M}_s(\mathcal{E}'_0)$ can potentially intersect transversally along a one-dimensional curve with $\mathcal{M}_u(\mathcal{E}'_i)$ in $\mathbb{R}^4$ for $i = 1$ and 3 [12, 13]. If this happens, then the existence of a heteroclinic connection between the equilibrium points $\mathcal{E}'_0$ and $\mathcal{E}'_i$ for $i = 1$ and 3 follows.

The linearization about $\mathcal{E}'_2$ leads to the following eigenvalues

$$\Lambda^4 - 2\,c\Lambda^3 - \gamma_1\Lambda^2 + \gamma_2\Lambda + \frac{\Delta + b\sqrt{\Delta}}{b + \sqrt{\Delta}} = 0,$$

and the corresponding eigenvalues $\dfrac{c \pm \sqrt{c^2 + 4\,d}}{2}$ and $\dfrac{c \pm \sqrt{c^2 - \frac{4}{d}\sqrt{\Delta}}}{2}$, where

$$\gamma_1 = \frac{\left(d^2\,b + \Delta - c^2d^2(d - \lambda\,k + \lambda\,A) - (c^2d + \lambda\,k - \lambda\,A)\sqrt{\Delta}\right)}{d\left(b + \sqrt{\Delta}\right)},$$

$$\gamma_2 = \frac{c\left(d^2\,b + \Delta + d^2b\sqrt{\Delta}\right)}{d\left(b + \sqrt{\Delta}\right)},$$

$\Delta = b^2 - 4\,d^2\,k\,\lambda$ and $b = d^2 + (k - A)\,\lambda$. Therefore, $\dim(\mathcal{M}_s(\mathcal{E}'_2)) = 3$ and $\dim(\mathcal{M}_u(\mathcal{E}'_2)) = 1$ with a critical speed $c^{**} = 2\sqrt{\dfrac{\sqrt{\Delta}}{d}}$ where $\Delta \geq 0$.

We summarize the result as follows.

Lemma 3. *Suppose that Case (b) of Proposition 1 holds, then*

$$dim(\mathcal{M}_s(\mathcal{E}'_2)) + dim(\mathcal{M}_u(\mathcal{E}'_3)) = dim(\mathbb{R}^4) + 1.$$

It should be noted that $\mathcal{E}'_2 = (0, S_2, 0, I_2)$ does not have zero components corresponding to the subpopulation densities. Therefore, it will be instructive to study oscillation of trajectories around this equilibrium point. For $0 < c < c^{**}$, which means travelling wave fronts travel with a speed smaller than the critical value c^{**}, there are two complex conjugate eigenvalues which lead to small oscillations in the travelling wave profiles around $\mathcal{E}'_2$. Numerical examples of heteroclinic orbits for all cases in Lemmas 1, 2 and 3 will be presented in Section 3.3.

3.2 Piecewise Constant Treatment Rate with a Jump

Here, we assume that the treatment rate is piecewise constant with a jump, i.e.,

$$T(I) = \begin{cases} m, & \text{if } I > 0, \\ \\ 0, & \text{if } I \leq 0. \end{cases} \tag{9}$$

(Case (ii)). Due to the discontinuity of $T(I)$, we cannot use our approach in section 3.1 to construct travelling waves. Further, we will see that the jump of $T(I)$ creates a jump in the second derivative of $v(z)$ and in the fourth derivative of $u(z)$ at $z = 0$. We claim the following result.

Theorem 4. *Suppose that we have Case (ii) for the treatment rate and that*

$$(\frac{\lambda\, A}{d} - d)v(z_0) > m \quad \textit{for some } z_0 > 0. \tag{10}$$

Then a positive travelling front solution $(u(z), v(z))$ of (7), if it exists, has the following properties: for all $c < 0$, $u(z)$ is monotone increasing for all $z \in (0, \infty)$ and $v(z)$ has at least one local maximum point $z_0 \in (0, \infty)$.

Proof. We first show that $u(z)$ is monotone increasing. Considering (7), we derive from the fact that $T(v)$ has a jump at $v = 0$, that v_{zz} has a jump where $v = 0$ and v, v_z are both smooth functions. Because of the jump for v_{zz} there is also a jump for u_{zzzz} and u, u_z, u_{zz}, u_{zzz} are all smooth functions.

Since $u(z) = \frac{A}{d}$ for $z < 0$, we derive $u(0) = A/d$ and $u_z(0) = u_{zz}(0) = u_{zzz}(0) = 0$. Using again (7), we derive $u_{zzzz}(0^+) = \dfrac{\lambda\, A\, m}{d}$. Thus,

$$u(z) = \frac{A}{d} + \frac{\lambda\, A\, m}{d}\frac{z^4}{24} + O(z^5) \text{ for } z > 0 \text{ small.}$$

This implies that $u(z) > \frac{A}{d}$ and $u(z)$ is increasing for z small enough. Suppose that $u(z)$ has a local maximum point z_0 with $u(z_0) > \dfrac{A}{d}$, then $u_z(z_0) = 0$ and $u_{zz}(z_0) \leq 0$. This implies that $f(z_0) = 0$ and $f_z(z_0) \leq 0$, but the right-hand side of (7b) is strictly positive (i.e., $c\, f - A + d\, u + \lambda\, u\, v > 0$) which is contradiction. Hence, $u(z)$ has no local maximum.

Next we show that $v(z)$ has at least one local maximum. Using again (7), we derive $v(0) = v_z(0) = 0$ and $v_{zz}(0^+) = m$. Therefore,

$$v(z) = m\frac{z^2}{2} + O(z^3) \quad \text{for } z > 0 \text{ small.}$$

Hence, $v(z)$ is monotone increasing for $z > 0$ small.

Assuming that $v(z)$ is monotone increasing for all $z > 0$ (i.e., $v(z_2) > v(z_1)$ for all $z_2 > z_1 > 0$) we will derive a contradiction. Then from (6b) we have for $z > z_0$

$$\begin{aligned} v_{zz} - c\,v_z &= -\lambda\,u\,v + d\,v + m \\ &\leq -\lambda\tfrac{A}{d}v + d\,v + m \quad \text{since } u \text{ is increasing (implying } u(z) \geq A/d) \\ &= v\left(-\lambda\tfrac{A}{d} + d\right) + m \\ &\leq v(z_0)\underbrace{\left(-\lambda\frac{A}{d} + d\right)}_{<0 \text{ by (10)}} + m \quad \text{since } v(z) > v(z_0) \text{ for all } z > z_0 \\ &\leq L < 0, \quad \text{where } L \text{ is a negative constant by (10).} \end{aligned}$$

Using that $v_{zz} - c\,v_z \leq L < 0$ for all $z > z_0$, we derive $g_z - cg \leq L$, where $g = v_z$. Setting $g(z) = \exp(cz)h(z)$, we have $h_z \exp(cz) \leq L$. Integrating this inequality gives $h(z) \leq -\frac{L}{c}\exp(-cz) + D$ for some real constant D. This implies $g(z) \leq -\frac{L}{c} + D\exp(cz) < 0$ for z large enough since $L < 0$. Integrating again, we get $v(z) = B_1\exp(c\,z) + B_2 - \dfrac{L}{c}z$ for some constants B_1, B_2. This implies that $v(z) < 0$ if z is large enough. This is a contradiction to the positivity of v. Therefore v is not monotone.

Since v is a continuously differentiable function which is monotone increasing for small enough $z > 0$ and monotone decreasing for some other $z > 0$, it must have a local maximum somewhere in between by the Intermediate Value Theorem for the derivative of $v(z)$.

□

Remark: The technical assumption (10) seems quite strong. However, we have not been able to prove the non-monotonicity or the existence of a local maximum for v without it.

Next we state a result about the behaviour of the solution as $z \to \infty$.

Theorem 5. *If $u(z) \to \infty$ and $v(z) \to 0$ as $z \to \infty$, then $u(z)\,v(z)$ approaches a constant.*

Proof. Let $u(z) \to \infty$ and $v(z) \to 0$, then $u(z)\,v(z) >> v(z)$, $u(z) >> u(z)\,v(z)$

and $u(z) >> A$ as $z \to \infty$. Thus, (7) in leading order reads

$$u_z = f, \tag{11a}$$

$$f_z = c\,f + d\,u \tag{11b}$$

$$v_z = g, \tag{11c}$$

$$g_z = c\,g - \lambda\,u\,v + m. \tag{11d}$$

From (11a) and (11b), we have $u_{zz} - cu_z - d\,u = 0$. Solving this linear equation for u, leads to the characteristic equation $\mu^2 - c\,\mu - d = 0$ which has the solutions

$$\mu_\pm = \frac{c \pm \sqrt{c^2 + 4\,d}}{2}.$$

Since $u(z) \to \infty$, we take

$$\mu_+ = \frac{c + \sqrt{c^2 + 4\,d}}{2}.$$

Further, considering the original system (7) we arrive at

$$u(z) = u_0 \exp(\mu_+\,z) + O(1) \quad \text{for some } z > 0, \tag{12}$$

since all the terms neglected when going from (7) to (11) are of order $O(1)$. This requires the estimate $v = O(\exp(-\mu_+\,z))$ which will be shown below.

We now determine the decay for v, assuming that $v(z) \to 0$ as $z \to \infty$. From (11c) and (11d), we obtain $v_{zz} - c\,v_z + \lambda\,u\,v - m = 0$. Substituting (12) into (11b) the $O(1)$ terms give $\lambda u\,v - m = 0$. Matching terms of the exact order $O(1)$, we derive $v(z) = H\exp(-\mu_+ z)(1 + o(1))$, where $H = \dfrac{m}{\lambda\,u_0}$. These are the same $O(1)$ terms as for the full system, given in (7).

Considering the terms of the exact order $O(\exp(-\mu_+\,z))$ in (7), we get $v_{zz} - c\,v_z - dv = O(\exp(-\mu_+\,z))$ as $z \to \infty$ (no resonance). Thus, for the solution of (7) we have the estimate

$$v(z) = H\exp(-\mu_+\,z) + O(\exp(-2\mu_+\,z)).$$

Hence, for the solution (u, v) of (7) we have derived the estimate $u(z)v(z) = \dfrac{m}{\lambda} + O(\exp(-\mu_+\,z))$. □

3.3 Numerical simulations

In this section, before mentioning our numerical results with regard to sections 3.1 and 3.2, it will be instructive to briefly describe the numerical methods used. For Case (i), since $T(I)$ is continuous, let $\xi = (\xi_1, \xi_1)$ and $\Phi = (\Phi_1, \Phi_1)$ be two equilibrium points we are interested in connecting. Then the travelling wave solutions, if they exist, must satisfy the following asymptomatic boundary conditions: $u(-\infty) = \xi_1$, $u(\infty) = \xi_2$ and $v(-\infty) = \Phi_1$, $v(\infty) = \Phi_2$. We truncate the interval $\mathbb{R} = (-\infty, \infty)$ by a finite interval $[Z_-, Z_+]$ where $Z_- < 0 < Z_+$ and $Z_\pm \in \mathbb{Z}$. We obtain the travelling wave solutions by simulating system (7) with $T(I)$ as defined in Case (i) as a Boundary Value Problem (BVP). We implemented this on MATLAB using solver *bvp4c* together with the projected boundary and phase conditions given by [42, 47, 48, 49]. By setting the truncated domain to be $[-30, 30]$, we use the following piecewise functions as initial conditions:

$$u(z) = \begin{cases} \xi_1, & \text{if } -30 \leq z \leq 0, \\ \\ \xi_2, & \text{if } 0 \leq z \leq 30, \end{cases} \qquad v(z) = \begin{cases} \Phi_1, & \text{if } -30 \leq z \leq 0, \\ \\ \Phi_2, & \text{if } 0 \leq z \leq 30. \end{cases} \tag{13}$$

Here, however, we do not fix the model variables and parameters throughout the simulations due to the existence conditions of the equilibrium points mentioned in Proposition 1. At first, we demonstrate the results for Theorem 3 with the following set of parameter values:

$$A = 2.8,\ \lambda = 0.001,\ r = 0.001,\ d = 0.02,\ k = 1. \tag{14}$$

This leads to $\mathcal{E}^{'}{}_0 = (0, 140, 0, 0)$ and $\mathcal{E}^{'}{}_1 = (0, 21, 0, 113.3333)$. Further, the condition for the existence of $\mathcal{E}^{'}{}_1$ is fulfilled (i.e., $p_0 = 6.345 < \mathcal{R}_0 = 6.6667 < p_2 = 51$, $\mathcal{R}_0 = 6.6667 < p_1 = 98.5714$). Figure 2 shows that there is no travelling wave front connecting the disease-free equilibrium $\mathcal{E}^{'}{}_0$ and the endemic equilibrium $\mathcal{E}^{'}{}_1$ with speed $c = 0.1099 < c^* = 0.6899$, because $v(z)$ takes negative values, which is unrealistic, and oscillates around the disease-free equilibrium $\mathcal{E}^{'}{}_0$. Hence, the simulation agreed with Theorem 3.

The subpopulation densities of susceptible individuals and infective individuals are represented as Subfigures $A1$ and $A2$ respectively, for most of the simulations. Figures 2 and 3 indicate that, as c decreases from c^*, more and more oscillations are observed.

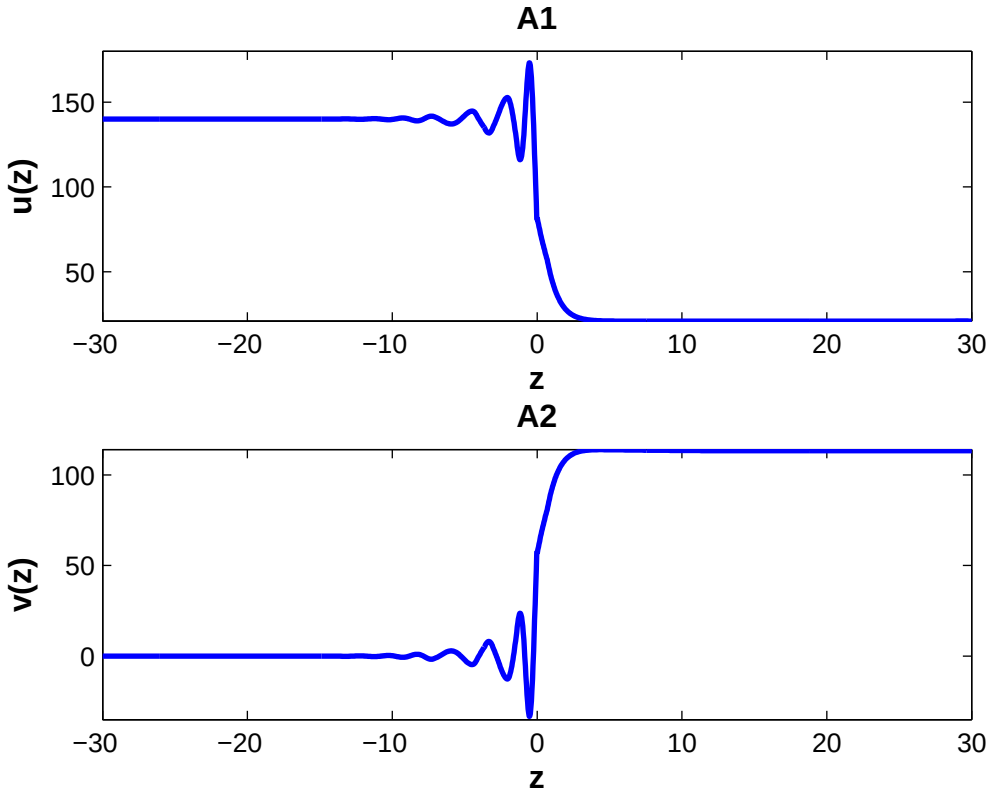

Figure 2: Assuming (14) with $c^* = 0.6899 > c = 0.1099$.

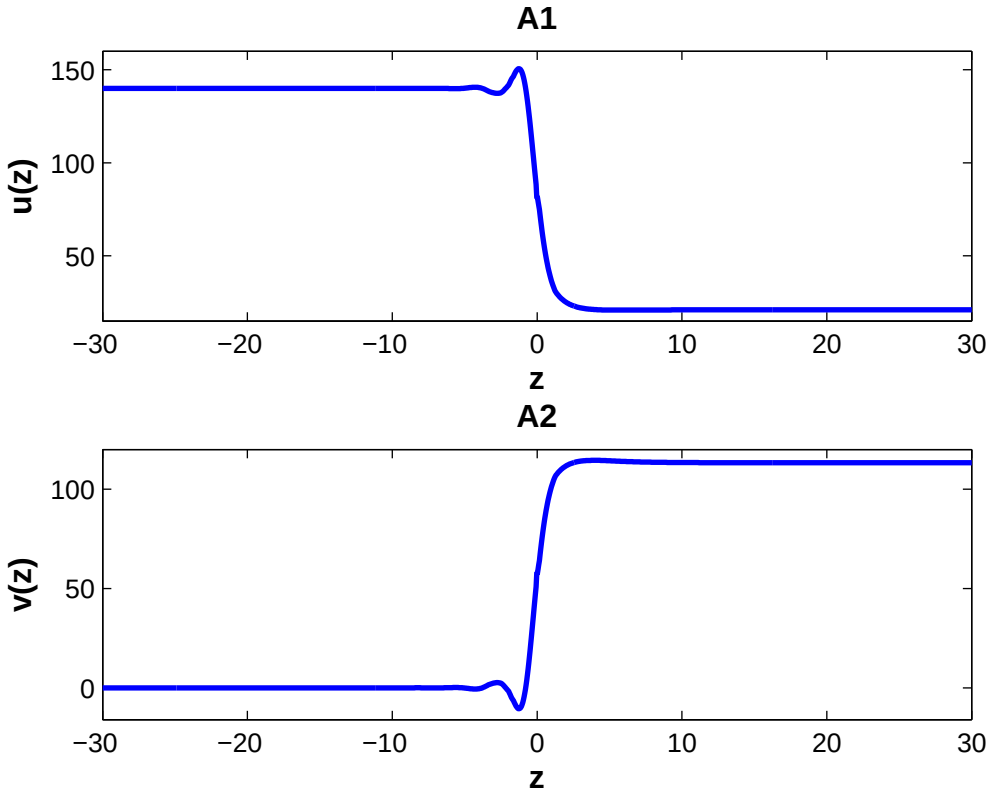

Figure 3: Assuming (14) with $c^* = 0.6899 > c = 0.2899$.

Now, we numerically illustrate the results obtained in Lemmas 1, 2 and 3, by carrying out some simulations. Lemma 1 suggests the connection between $\mathcal{E}'_0$ and $\mathcal{E}'_1$ and we have the following:

$\Delta_2 \geq 0$: all the eigenvalues of the jacobian evaluated at $\mathcal{E}'_1$ are strictly real and hence smooth travelling wave profiles, corresponding to the system (7) with $T(I)$ as defined in Case (i), connecting $\mathcal{E}'_0$ and $\mathcal{E}'_1$ are obtained as depicted in Figure 4.

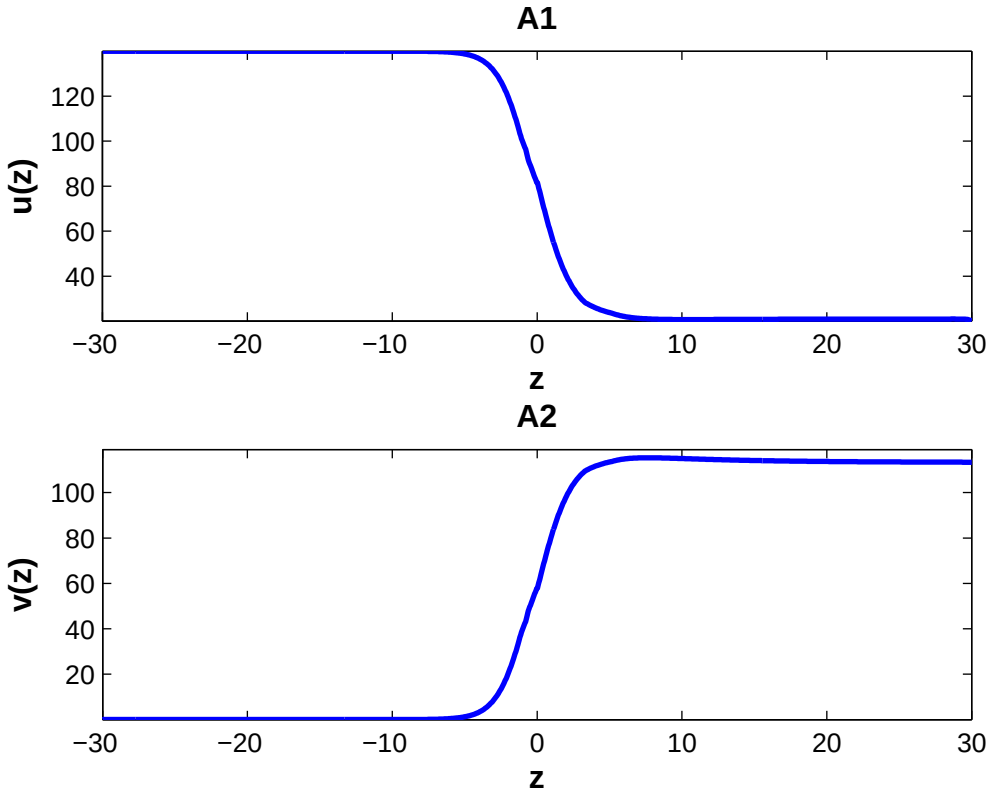

Figure 4: Assuming (14) with $\Delta_2 = 0.0083$ and $c = 0.9899$.

$\Delta_2 < 0$: non-monotone travelling wave solutions connecting $\mathcal{E}'_0 = (0, 140, 0, 0)$ and $\mathcal{E}'_1 = (0, 30, 0, 73.3333)$ are obtained as shown in Figure 5. Here, we observed a hump in the wave profile for $v(z)$ and a corresponding dip in that for $u(z)$.

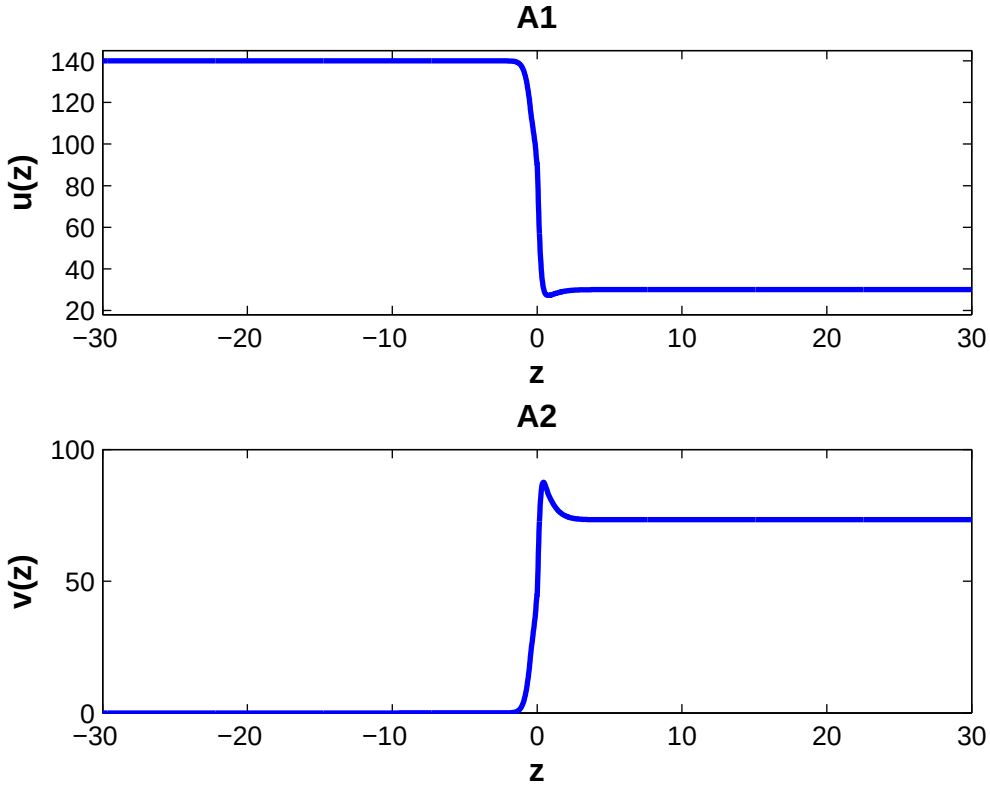

Figure 5: Assuming (14) with $r = 0.01$ and $c = 0.6643$. This leads to $\Delta_2 = -8.8889 \cdot 10^{-5}$, $p_0 = 4.4415 < \mathcal{R}_0 = 4.6667 < p_2 = 6$, $\mathcal{R}_0 = 4.6667 < p_1 = 9$.

Lemma 2 suggests the connection between $\mathcal{E}'_0$ and $\mathcal{E}'_3$ and Figure 6 depicts non-monotone wave fronts connecting the two equilibria. This shows a zone of transition from the disease-free equilibrium $\mathcal{E}'_0$ to the endemic equilibrium $\mathcal{E}'_3$ where the level of susceptible individuals first decreased and then increased, and that of infective individuals first increased then decreased.

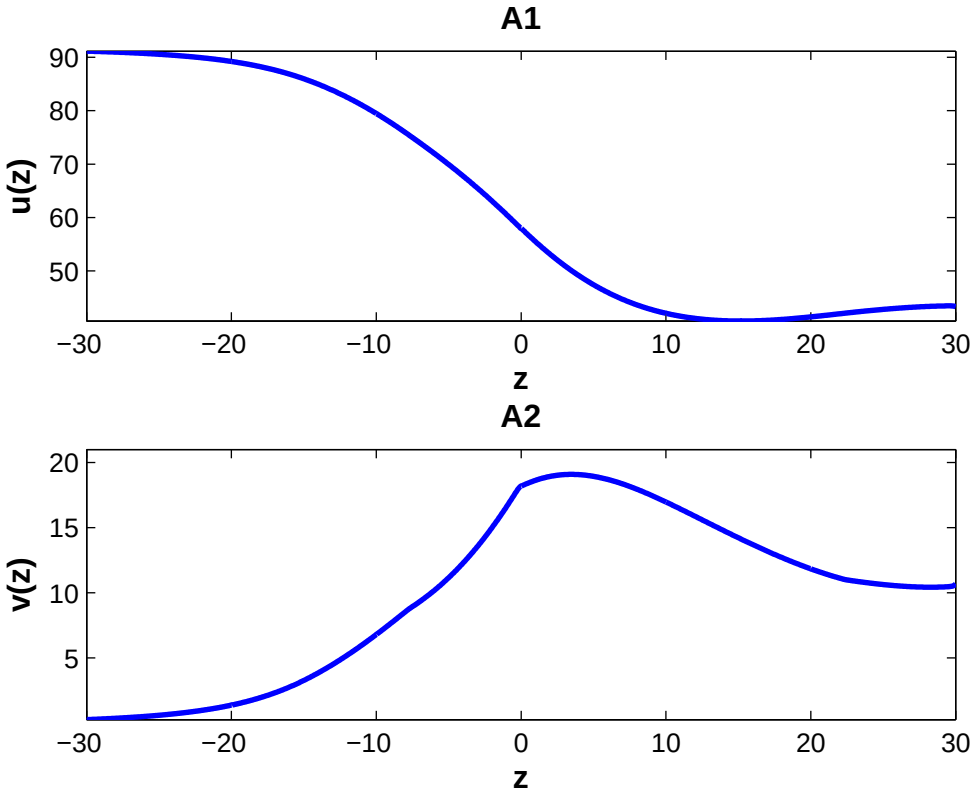

Figure 6: $\mathcal{E}'_0 = (0, 91.6, 0, 0)$, $\mathcal{E}'_3 = (0, 44.4788, 0, 11.7712)$, $\mathcal{R}_0 = 1.8320$, $\Delta = 3.7779 \cdot 10^{-8}$, $p_0 = 1.7220$, $p_1 = 1.3332$, $p_2 = 1.9090$, $A = 0.916$, $\lambda = 0.0009$, $r = 0.035$, $d = 0.01$, $I_0 = 10.1$.

Lemma 3 suggests the connection between $\mathcal{E}'_2$ and $\mathcal{E}'_3$ if Case (b) of Proposition 1 holds (i.e., $\mathcal{E}'_2$ and $\mathcal{E}'_3$ exist simultaneously). Thus, the model parameters and variables are fixed as follows:

$$A = 0.916,\ \lambda = 0.003,\ r = 0.035,\ d = 0.02,\ k = 0.35. \tag{15}$$

The conditions for the existence of $\mathcal{E}'_3$ and $\mathcal{E}'_3$ are satisfied (i.e., $p_0 = 2.4965 < \mathcal{R}_0 = 2.4982 < p_2 = 2.5$ $\mathcal{R}_0 = 2.4982 > p_1 = 2.4091$). We investigate the travelling wave solutions connecting $\mathcal{E}'_2 = (0, 18.0609, 0, 10.2391)$ and $\mathcal{E}'_3 = (0, 16.9057, 0, 11.3943)$ as follows:

If $c \geq c^{**}$ then there are travelling wave profiles which connect $\mathcal{E}'_2$ and $\mathcal{E}'_3$ without any oscillations as depicted in Figure 7. The wave profiles for both $u(z)$ and $v(z)$ are monotone and smooth.

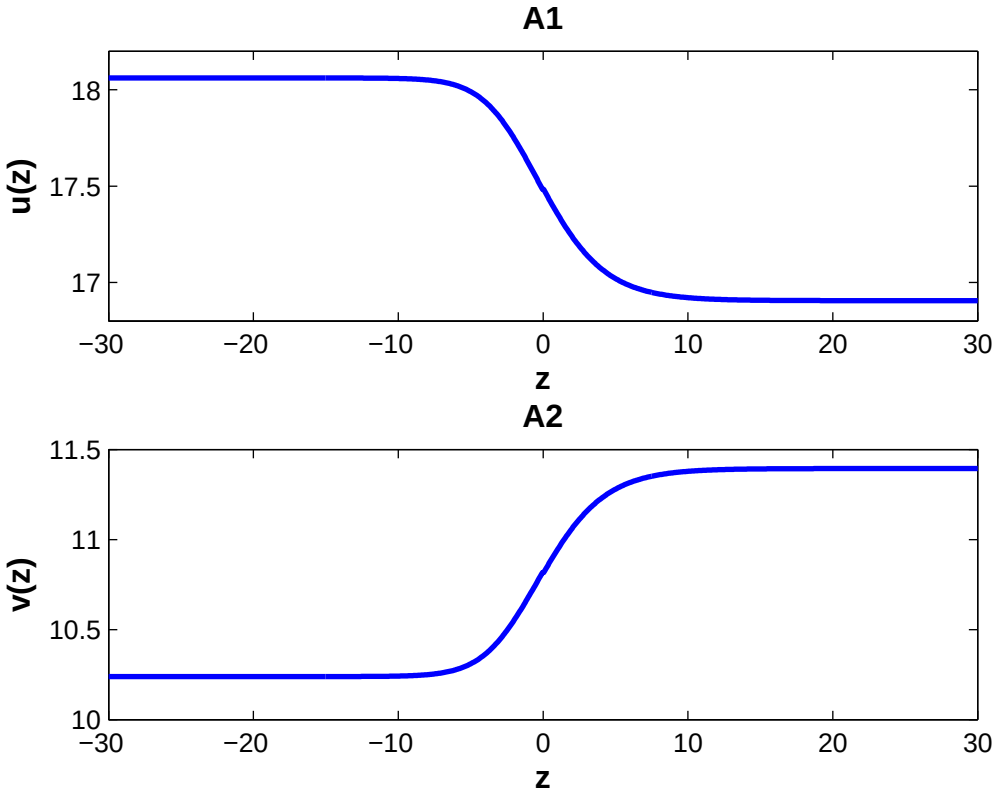

Figure 7: Assuming (15) with $\Delta = 4.8040 \cdot 10^{-9}$, $c^{**} = 0.1177 < c = 0.1277$

If $c < c^{**}$ then there is a travelling wave profile connecting $\mathcal{E}'_2$ and $\mathcal{E}'_3$ which oscillates near $\mathcal{E}'_2$ as shown in Figure 8.

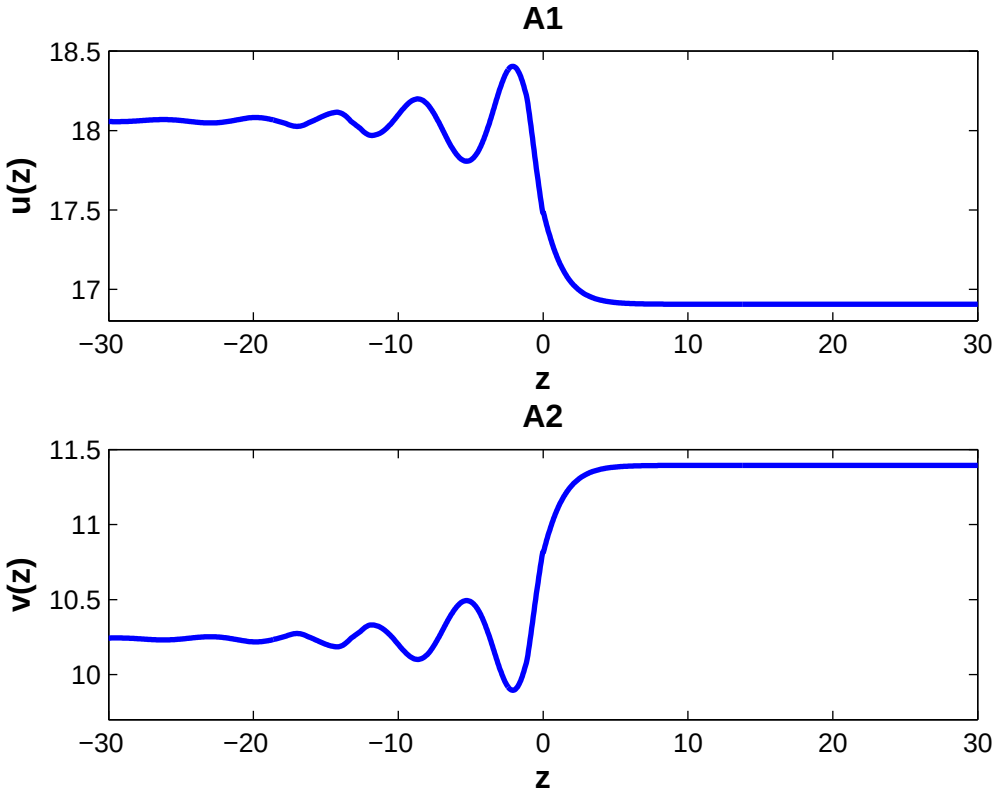

Figure 8: Assuming (15) with $\Delta = 4.8040 \cdot 10^{-9}$, $c^{**} = 0.1177 > c = 0.0176$.

Finally, we consider system (7), with $T(I)$ defined in Case (ii), as Initial Value Problem (IVP) with initial condition $(A/d, 0, 0, 0)$ due to the discontinuity of $T(I)$. We show the results obtained in Theorems 4 and 5, by carrying out some simulations as depicted in Figures 9(A & B) and 9C respectively. The observed behaviour of the system is qualitatively different from that of the case analysed previously, and the travelling wave connects the disease-free equilibrium state to another disease-free state for which $u \to \infty$. In the last part of Figure 9 it can be seen that $u(z)v(z) \to \frac{m}{\lambda} = 110$ (compare with the proof of Theorem 5).

It is evident from Figure 10 that the travelling wave profile for the density of the infective individuals $v(z)$ oscillates in the initial phase as the removal rate of the infective individuals m increases. Furthermore, the decay rate of $v(z)$, as calculated in Theorem 9C, is independent of the removal rate m. It can be read off that the gradient of $\log(v(z))$ approaches approximately 0.03 which corresponds reasonably well with the

value $\mu_+ \approx 0.06$ for the approximate solution (see the proof of Theorem 5).

With increasing removal rate m of the infective individuals, the region where the disease presents high incidence shrinks, and the maximum of $v(z)$ increases with m.

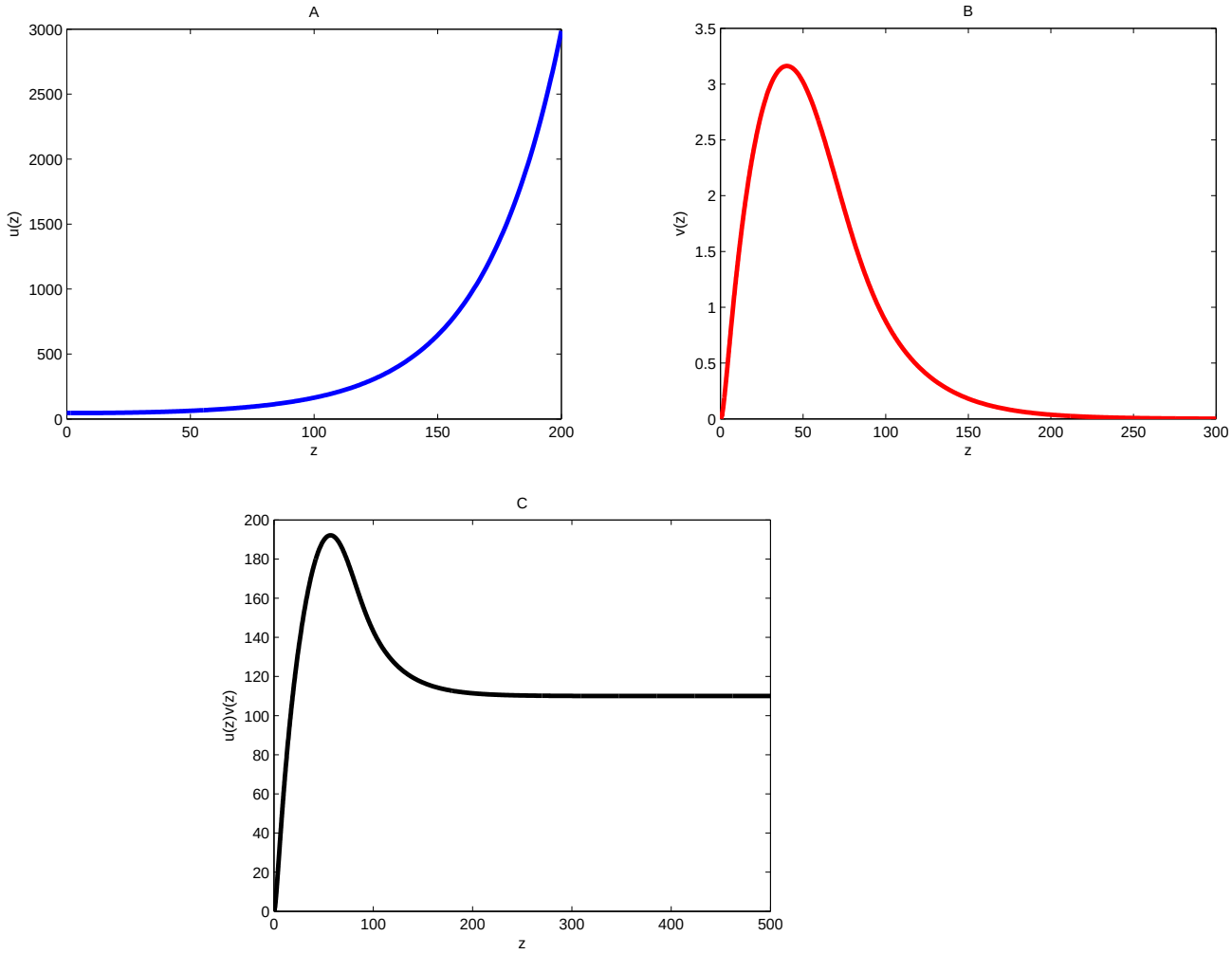

Figure 9: $A = 0.916$, $d = 0.02$, $\lambda = 0.001$, $m = 0.11$, $c = -0.6$.

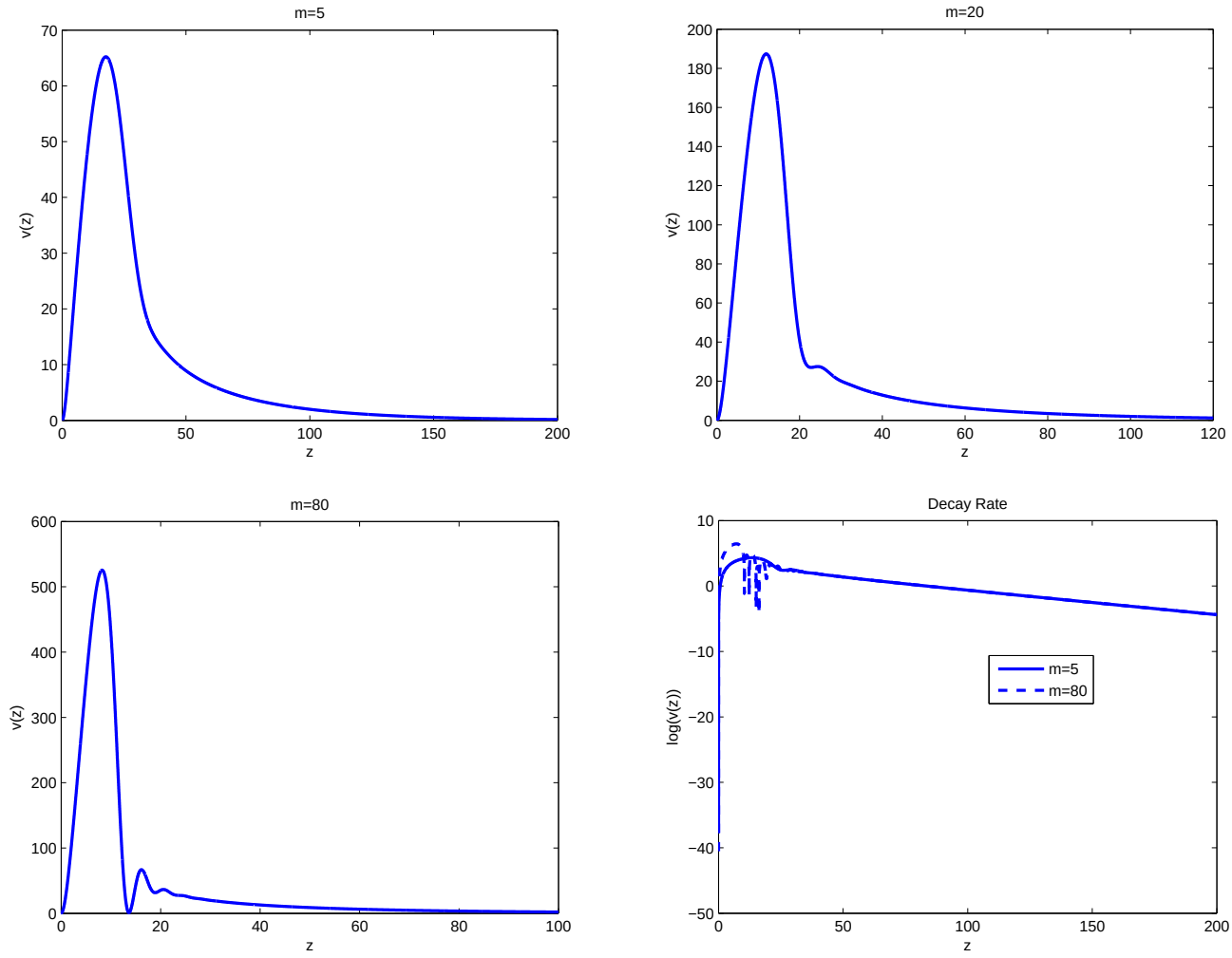

Figure 10: $A = 1$, $d = 0.02$, $\lambda = 0.001$, $c = -0.5$

4 Conclusion

In this work, we incorporate reaction-diffusion terms in a simplified form of the systems in [5] and [10] to model the spatial spread of an epidemic in the presence of a treatment in a given populations. This work has been motivated by our effort to analyze the effect of the nature of treatment rate in the model. That is, nonlinear and non-smooth treatment terms; namely, (i) piecewise linear treatment rate with saturation effect, (ii) piecewise constant treatment rate with jump (Heaviside function). We have analyzed the linear stability of the disease-free equilibrium of the model with both treatment terms. Travelling waves are constructed and their existence is numerically shown in

both cases. Furthermore, when the treatment rate is piecewise linear with saturation effect we have shown that there are travelling wave trajectories which connect the disease-free state to an infective state and also between two endemic states, while with piecewise constant rate of treatment, which has a jump at the disease-free state, we can only connect the disease-free state to itself. Biologically, the latter is indeed of public health importance because it shows that if few infectives are introduced into a completely susceptible population, then there will be a moving transition zone of high concentration of infective individuals only for a while, and the infectives vanish at the end of the wave front. However, the former demonstrates the conditions of reaching an endemic state from the disease-free state and how two infective states are connected. For piecewise linear treatment rate with saturation effect, we observe some phenomena which are not present for travelling-waves in classical SIR systems with constant coefficients such as non-monotone profiles for both susceptibles and infectives, or oscillations of the profiles due to complex eigenvalues. However, if the treatment rate is piecewise constant and has a jump, the wave profile for susceptible individuals tends to infinity, whilst the infectives converge to zero and their product approaches a constant at the forward end of the profile. For increasing removal rate m of the infective individuals oscillations of the wave profile occur and their amplitude increases.

In model (3), it would be desirable to study the stability of travelling waves. Further, it is instructive to investigate the spatial spread in higher-dimensional space. The mathematical analysis for the resulting model is considerably more complicated and so, we leave it for future work. Furthermore, our assumption that susceptible individuals and infectives diffuse at the same rate is not necessary, one could also study the effects of different diffusion rates on the travelling wave profile.

References

[1] W.O. Kermack, A.G. McKendrick, A contribution to the mathematical theory of epidemics, *Proc. R. Soc. London*, 115 (1927), 700–721.

[2] H.W. Hethcote, Three basic epidemiological models, in: S.A. Levin, T.G. Hallam, L. Gross (Eds.), Applied Mathematical Ecology. Biomathematics, vol. 18, Springer, Berlin, 1989.

[3] H.W. Hethcote, The mathematics of infectious diseases, *SIAM Rev.*, 42 (2000) 599–653.

[4] M.A. Fuentes, M.N. Kuperman, Cellular automata and epidemiological models with spatial dependence, *Physica A* 267 (1999) 471–486.

[5] W. Wang and S. Ruan, Bifurcations in an epidemic model with constant removal rate of the infectives, *J. Math. Anal. Appl.*, 291 (2004) 775–793.

[6] R.M. May, R.M. Anderson, Population biology of infectious diseases, part II, *Nature* 280 (1979) 455–461.

[7] M.J. Keeling, P. Rohani, B.T. Grenfell, Seasonally forced disease dynamics explored as switching between attractors, part II, *Physica D*, 148 (2001) 317–335.

[8] M. Altmann, Susceptible-infective-removed epidemic models with dynamic partnerships, *J. Math. Biol.* 33 (1995) 661–675.

[9] Q. X. Liu and Z. Jin, Formation of spatial patterns in an epidemic model with constant removal rate of the infectives, *J. Stat. Mech.*, (2007) P05002.

[10] W. Wang, Backward bifurcation of an epidemic model with treatment, *Mathematical Biosciences*, 201 (2006) 58–71.

[11] J. Smoller, Shock Waves and Reaction-Diffusion Equations, 2nd ed., Springer-Verlag, New York, 1994.

[12] P.B. Ashwin, M.V. Bartuccelli, T.J. Bridges, S.A. Gourley, Travelling fronts for the KPP equation with spatio-temporal delay, *Z. Angew. Math. Phys.*, 53 (2002) 103-122.

[13] J. Guckenheimer, P. Holmes, Nonlinear Oscillations, Dynamical Systems, and Bifurcations of Vector Fields, Applied Mathematical Sciences, vol. 42, Springer, 1983.

[14] A. d'Onofrio, P. Manfredi, E. Salinelli, Vaccinating behaviour, information, and the dynamics of SIR vaccine preventable diseases, *Th. Pop. Biol.*, 77 (2007), 301–317.

[15] R. Gardner, Review on Traveling Wave Solutions of Parabolic Systems by A. I. Volpert, V. A. Volpert and V. A. Volpert, *Bull. Am. Math. Soc.*, 32 (1995), 446–452.

[16] P. C. Fife, Mathematical Aspects of Reaction and Diffusion System Lecture Notes in Biomathematics, Vol. 28, Springer-Verlag, New York. 1979.

[17] R.M. Anderson, R.M. May, Infectious Diseases of Humans: Dynamics and Control, Oxford University Press, Oxford, 1991.

[18] J.D. Murray, Mathematical Biology II, 3rd ed., Springer-Verlag, Berlin, 2003.

[19] L. Rass, J. Radcliffe, Spatial Deterministic Epidemics: Mathematical Surveys and Monographs, vol. 102, American Mathematical Society, Providence, Rhode Island, 2003.

[20] C. Conley, Traveling wave solutions of nonlinear diffusion equations, Springer Lecture Notes in Physics, No. 38, Springer-Verlag, New York, 1975.

[21] F. van den Bosch, J.A.J. Metz, O. Diekmann, The velocity of spatial population expansion, *J. Math. Biol.*, 28 (1990) 529–565.

[22] C. Conley, R. Gardner, An application of the generalized Morse index to traveling wave solutions of a competitive reactiondiffusion model, *Indiana Univ. Math. J.*, 44 (1984) 319-343.

[23] S.R. Dunbar, Travelling wave solutions of diffusive LotkaVolterra equations: a heteroclinic connection in R^4, *Trans. Amer. Math. Soc.*, 268 (1984) 557-594.

[24] E. D. Conway, J. A. Smoller, Diffusion and the Predator-Prey Interaction, *SIAM Journal on Applied Mathematics*, 33 (1977) 673–686.

[25] E. D. Conway, J. A. Smoller, A Comparison Technique for Systems of Reaction-Diffusion Equations, *Comm. in Part. Differ. Equations*, 2 (1977) 679–698.

[26] A.I. Volpert, V.A. Volpert, V.A. Volpert, Traveling Wave Solutions of Parabolic Systems, in: Translations of Mathematical Monographs, vol. 140, American Mathematical Society, Providence, 1994.

[27] G. F. Webb, A recovery-relapse epidemic model with spatial diffusion, *Journal of Mathematical Biology*, 14 (1982) 177–194.

[28] P. Marcati, M. A. Pozio, Global asymptotic stability for a vector disease model with spatial spread, *Journal of Mathematical Biology* 9 (1980) 179–187.

[29] J. Rauch, J. Smoller, Qualitative theory of the FitzHugh-Nagumo equations, *Advances in Mathematics*, 27 (1978) 12–44.

[30] R. Gardner, J. Smoller, The existence of periodic travelling waves for singularly perturbed predator-prey equations via the Conley Index. *Journal of Differential Equations*, 47 (1983) 133–161.

[31] M. Mimura, Asymptotic Behaviors of a Parabolic System Related to a Planktonic Prey and Predator Model, *SIAM Journal on Applied Mathematics*, 37 (1979) 499–512.

[32] J. Arino, F. Brauer, P. van den Driessche, J. Watmough, J. Wu, A model for influenza with vaccination and antiviral treatment, *Math. Biosci. Eng.*, 5 (2008) 118-30.

[33] F. Brauer, Epidemic Models with Heterogeneous Mixing and Treatment, *Bulletin of Mathematical Biology*, 70 (2008) 1869–1885.

[34] Z. Gul, Y.H. Kang, I.H. Jung, Optimal treatment of an SIR epidemic model with time delay, *Biosystems*, 98 (2009) 43–50.

[35] J.M. Hyman, J. Li, Modeling the effectiveness of isolation strategies in preventing STD epidemics, *SIAM J. Appl. Math.*, 58 (1998) 912-925.

[36] E. Jung, S. Lenhart and Z. Feng, Optimal control of treatments in a two-strain tuberculosis model, *Discrete and Continuous Dynamical Systems-Series B* 4 (2002) 473-482.

[37] A.B. Gumel, S. Ruan, T. Day, J. Watmough, F. Brauer, P. van den Driessche, D. Gabrielson, C. Bowman, M.E. Alexander, S. Ardal, J. Wu, and B.M. Sahai, Modelling strategies for controlling SARS outbreaks, *Proc R Soc B*, 271 (2004) 2223–2232.

[38] X. Yan, Y. Zou, Optimal and sub-optimal quarantine and isolation control in SARS epidemics, *Mathematical and Computer Modelling*, 47 (2008) 235 – 245.

[39] P. Hartman, Ordinary Differential Equations, Wiley, NewYork, 1973.

[40] G. Mulone, B. Straughan, and W. Wang, Stability of Epidemic Models with Evolution, *Studies in Applied Mathematics*, 118 (2007) 117–132.

[41] G. Mulone, and B. Straughan, Nonlinear Stability for Diffusion Models in Biology, *SIAM Journal on Applied Mathematics*, 69 (2009) 1739–1758.

[42] W.-J. Beyn, The numerical computation of connecting orbits in dynamical systems, *IMA Journal of Numerical Analysis*, 9 (1990) 379-405.

[43] S. Ruan, and W. Wang, Dynamical behavior of an epidemic model with a nonlinear incidence rate, *J. Differential Equations* 188 (2003) 135-163.

[44] G. Sun, Z. Jin, Q. Liu and L. Li, Pattern formation in a S-I model with nonlinear incidence rates, *J. Stat. Mech.* (2007) P11011.

[45] W. Wang, X. Zhao, An epidemic model with population dispersal and infection period, *SIAM J. Appl. Math.* 66 (2006) 1454-1472.

[46] G. Sun, Z. Jin, Q. Liu and L. Li, Chaos induced by breakup of waves in a spatial epidemic model with nonlinear incidence rate, *J. Stat. Mech.* (2008) P08011.

[47] W.-J. Beyn, Global bifurcations and their numerical computation Continuation and Bifurcations: Numerical Techniques and Applications, Dordrecht, Netherlands, 1990.

[48] A.R. Champneys, Y.A. Kuznetsov, and B. Sandstede, A numerical toolbox for homoclinic bifurcation analysis, *International Journal of Bifurcation and Chaos*, 6 (1996) 867-887.

[49] F. Bai, A. Spence and A.M. Stuart, The Numerical Computation of Heteroclinic Connections in Systems of Gradient Partial Differential Equations, *SIAM Journal on Applied Mathematics*, 53 (1993) 743-769.